

# Electron Microscopic Observations of SiO<sub>2</sub> Precipitates at Dislocations in Silicon

D. BIALAS, J. HESSE

*AEG-Telefunken, Forschungsinstitut, Frankfurt am Main, Germany*

*Received 3 March 1969*

The precipitation of oxygen from silicon single crystals has been examined. It has been found that oxygen precipitates are formed preferentially at dislocations. This finding enabled the formation of zones with high particle density and with large particles, which aided identification. It was then shown that the precipitates consisted of crystalline  $\alpha$ - and  $\beta$ -SiO<sub>2</sub> grown in a manner partially coherent with the Si lattice. Some of the precipitates are hexagonal prisms with the longitudinal axis in the  $\langle 110 \rangle$  direction of the Si-matrix.

## 1. Introduction

The physical properties of oxygen-rich silicon are changed by heat-treatment [1-10]. This is explained, amongst other things, by the formation of oxygen precipitates. In particular the formation of new donor centres in the temperature range between 400 and 600° C, observed by Fuller and Logan [11], has been explained by Kaiser and co-workers [12] in this way. From the disappearance of the absorption band at 9  $\mu$ m in the infra-red spectrum above 1000° C, Kaiser [2] has concluded that oxygen precipitates are present in the form of SiO-complexes. Their existence has in fact been proved both by X-ray radiography [10] and also by means of the scanning electron microscope [13], but their structure could not be clarified because the number and magnitude of the particles was too small, even in samples with an above equilibrium vacancy concentration. According to [14] vacancies can act as nuclei for oxygen precipitation. Using the same temperature processing as [14] which leads to noticeable changes in the 9  $\mu$ -band, we observed, with the electron microscope, only a few small particles which proved inadequate for identification. It was decided to attempt to induce the formation of larger precipitates by other means. For copper in silicon it is well known that precipitates form preferentially at dislocations [15-17]; hence it was considered reasonable to look for oxygen precipitation in

samples of silicon which had both a very large dislocation density and a high oxygen content.

## 2. Experimental

In order to produce a high dislocation density, we have used the fact that elastic strains introduced into silicon at room temperature will be released at high temperatures with the formation of dislocation networks. Such elastic strains can arise for example, due to mechanical working of the sample [18], (in this case by sawing). The resulting dislocation density ranged from about 10<sup>7</sup> to 10<sup>8</sup> cm<sup>-2</sup>, both near the surface and down to depths of some  $\mu$ m, being thus comparable in magnitude to the dislocation density in germanium, necessary to form lithium precipitates at similar dislocations [19].

The high oxygen content, required near the dislocations (i.e. near the surface of the sample), was produced by indiffusion of oxygen. The thermal treatment, necessary for forming the dislocations was performed in an oxygen atmosphere.

The detection and identification of the precipitates was carried out using an electron microscope. For this purpose the samples were thinned chemically after the heat-treatment and observed in transmission with an electron microscope type JEM 150.

The investigations were performed on zone refined n-type silicon single crystals having an

electrical resistivity of  $40 \Omega\text{cm}$ .  $200 \mu\text{m}$  thick slices were cut with a diamond saw from larger, single crystals perpendicular to the  $\langle 111 \rangle$  growth direction, and then smaller discs with a diameter of  $3 \text{ mm}$  were bored out with an ultrasonic drill. The subsequent annealing was performed at  $1000^\circ \text{C}$  in an oxygen atmosphere for times of 3 to 160 h. The superficial oxide film which was formed was dissolved with hydrofluoric acid and the samples were thinned chemically by means of the jet-etch process, described by Booker and Stickler [20]. The rough surface of the sample, resulting from sawing, proved advantageous due to the numerous small holes which were formed enlarging the field of view obtained with the electron microscope.

### 3. Results

The electron microscope picture of a sample, diffusion-annealed for 24 h at  $1000^\circ \text{C}$  in an oxygen atmosphere, is shown in fig. 1. A dislocation network is formed, reaching down 5 to  $7 \mu\text{m}$  under the initial surface of the sample. The dislocations lie preferentially parallel to the  $\langle 110 \rangle$  direction of the silicon lattice and it can be seen that precipitates have in fact formed at these dislocations. In plan view their geometric form is often hexagonal, as may be seen in magnified display in fig. 2a. The boundary lines coincide with the  $\langle 110 \rangle$  directions. Further, in order to inspect the form of the precipitates shown in fig. 2a, perpendicular to the  $\{111\}$  plane, we investigated samples oriented parallel

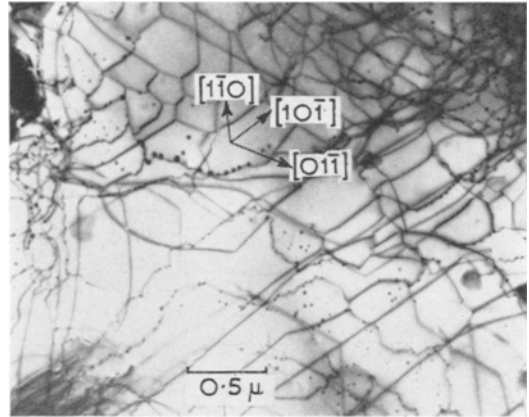


Figure 1 Dislocation network in silicon, decorated with  $\text{SiO}_2$  precipitates.

to the  $\langle 111 \rangle$  direction. The result is shown in fig. 2b. In conjunction with fig. 2a it is clear that hexagonal prisms have been formed. They are crystalline and this has been confirmed by dark-field observation and changing the orientation contrast by tilting the sample. Contrast changes in the immediate vicinity of the particles, which would have suggested a distortion of the silicon matrix by the precipitates, have not been found for the large precipitates, shown in figs. 2a and 2b. They appear only at the start of precipitation with very small particles.

Besides the precipitations in the immediate neighbourhood of a dislocation, precipitates arranged in rows and without immediate connection with a dislocation site have also been

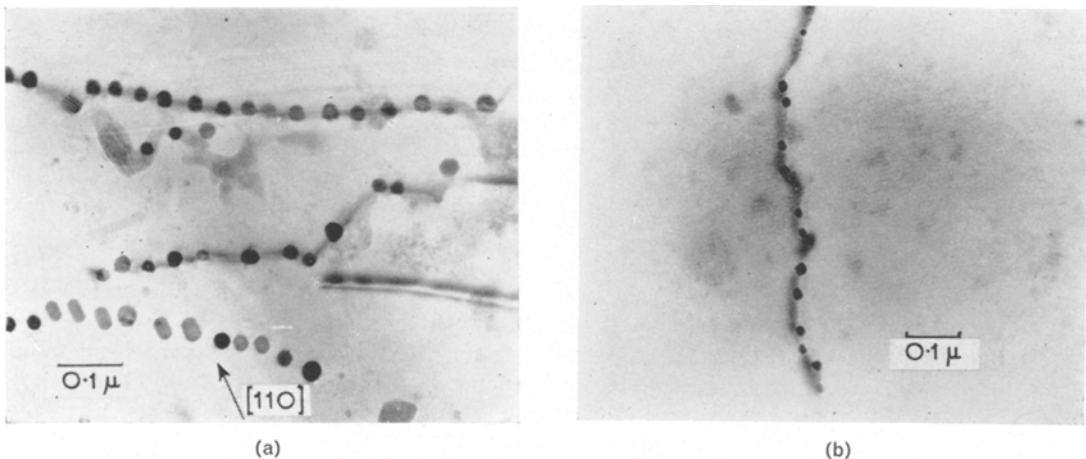


Figure 2  $\text{SiO}_2$  precipitates. (a) Image plane parallel to the  $\{111\}$  plane in Si (b) image plane perpendicular to the  $\{111\}$  plane of the Si.

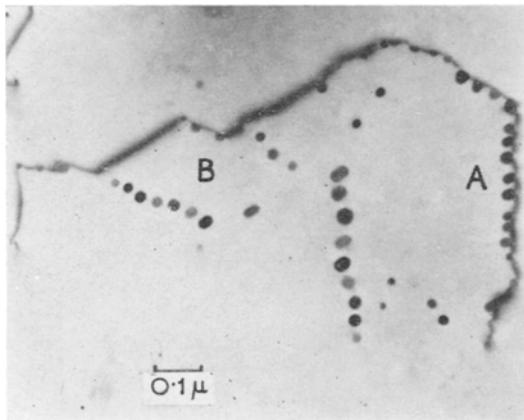
observed (fig. 3a). Usually in these cases, a geometrical assignment to a dislocation, located nearby, from which these precipitates had obviously been severed, was possible. The configuration, marked with an A in fig. 3a, shows that the force, acting on the dislocation, drives these away from the precipitations. Furthermore, it seems to be possible that vacancies left from non-conservative movement of jogs in screw dislocations can also act as nuclei for precipitates. The configuration, marked with a B in fig. 3a, leads to this assumption. Rieger [17] has also explained the precipitation of copper in silicon in this way. Further, in agreement with Rieger [17] we also observed regions with high particle density bounded by dislocations (fig. 3b). In [17] this was explained by repulsive stresses set up in the silicon matrix by the precipitations, which drive the dislocations away from the precipitations. This could not hold for oxygen in silicon. On the contrary, the larger particles would, rather, be obstacles for the motion of the dislocations as demonstrated in fig. 3a (A). It seems to be more likely that these arrays are formed stepwise during expansion of the dislocation loop.

The large particles in the vicinity of the dislocations facilitated the electron diffraction analysis. The measured interlattice plane distances of the precipitates are compiled in the table given below. A comparison with the known  $d$ -values for  $\alpha$ - and  $\beta$ -SiO<sub>2</sub> leads to the conclusion that in the precipitates,  $\alpha$ - as well as  $\beta$ -SiO<sub>2</sub> must be included, because only then can all the measured  $d$ -values be correlated. Because of the

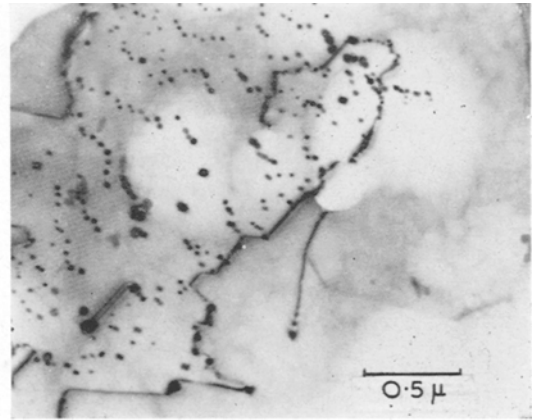
TABLE I Identification of measured interlattice plane distance.

$d_{exp}$ Å	$d_{\alpha-SiO_2}$ Å	$d_{\beta-SiO_2}$ Å
—	4.260	4.43
$3.38 \pm 0.05$	3.343	3.42
2.54	—	2.55
2.45	2.458	—
2.31	—	2.30
2.27	2.282	—
2.245	2.237	—
2.22	—	2.22
2.12	2.128	—
2.04	—	2.05
1.99	1.980	—
1.845	—	1.85
1.82	1.817	—
1.81	1.801	—
1.73	—	1.71
1.665	{ 1.672 1.659	—
1.63	1.608	—
1.56	—	1.57
1.545	1.541	—
1.47	1.453	—
1.425	1.418	1.42
1.41	{ 1.382 1.375	1.39
1.35	1.372	—
1.30	1.288	1.29
1.25	1.256	{ 1.277 1.225

higher intensity observed for the diffraction patterns of the  $\beta$ -SiO<sub>2</sub> one may conclude, that the  $\beta$ -phase prevails. According to the silicon oxygen phase-diagram the  $\beta$ -phase is stable only



(a)



(b)

Figure 3 Areas of precipitations limited (a) on one side or (b) on all sides by dislocations.

above 577° C and it follows that in this case the  $\beta$ -phase is in the metastable form.

The  $\text{SiO}_2$  precipitates, identified by means of electron diffraction, form moiré patterns, as may be seen in fig. 4. A means therefore exists by

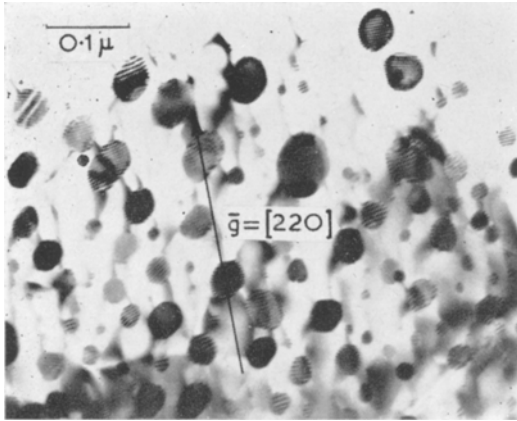


Figure 4  $\text{SiO}_2$  precipitates with moiré structure.

which the correctness of the identification can be checked and from which conclusions on the coherence of the particles can be drawn. Moiré patterns are formed by interference effects in two crystals lying one upon the other, either if the lattice plane systems lie parallel to one another with slightly different lattice spacings  $d_1$  and  $d_2$  (parallel moiré patterns), or if, with equal values of  $d$ , the lattice planes are at an angle ( $\gamma$ ) to one another (rotational moiré patterns) [21]. In general form the pattern spacing  $D$  is given by:

$$D = \frac{d_1 d_2}{(d_1^2 + d_2^2 - 2d_1 d_2 \cos \gamma)^{1/2}} \quad (1)$$

From fig. 4 it follows that the patterns lie predominantly perpendicular to the diffraction vector  $\mathbf{g} = \langle 220 \rangle$ . From the deviation,  $\phi$ , of the direction of the moiré patterns from 90° to the  $\mathbf{g}$ -vector, the angle of deviation of the reflection lattice planes of the precipitates with respect to the  $\{220\}$  planes of the silicon may be computed according to

$$\sin \phi = \frac{D}{d_2} \sin \gamma \quad (2)$$

It was found that the angle  $\gamma$  was smaller than  $\pm 1^\circ$  in 95% of all precipitates investigated. Hence it follows that parallel moiré patterns are present ( $\gamma \approx 0$  in (1)). The distance  $D$  of the patterns is measured in fig. 4. The spacing of the

$\{220\}$  planes of silicon is  $d_1 = 1.920 \text{ \AA}$ , so that the required spacing  $d_2$  of the reflecting lattice planes of the precipitates can be computed. It is found that  $d_2 = 1.843 \text{ \AA}$  and this is in good agreement with the spacing of the  $\{112\}$  planes of  $\beta\text{-SiO}_2$ , which is  $d = 1.850 \text{ \AA}$ . For  $\alpha\text{-SiO}_2$  the value found could be assigned to the  $\{212\}$  lattice plane spacing ( $d = 1.870 \text{ \AA}$ ). Hence the results prove the validity of the hypothesis that the precipitates are mainly  $\beta\text{-SiO}_2$ .

The orientation relations found by analysis of the moiré structures also enable one to draw conclusions about the coherence of the  $\beta\text{-SiO}_2$  particles. If their  $\{112\}$  planes are parallel to the  $\{110\}$  planes of the silicon, then the planes of the silicon, perpendicular to them, are the  $\{111\}$  planes with  $d = 3.138 \text{ \AA}$  and in  $\beta\text{-SiO}_2$  the  $\{211\}$  planes with  $d = 1.570 \text{ \AA}$ , the deviation from 90° being about 4°. Neglecting this small discrepancy, one obtains a good matching with the silicon lattice by doubling the value for  $d$  of the  $\{211\}$  planes of the  $\text{SiO}_2$ . From this it follows that the precipitates are partially coherent.

#### 4. Conclusions

It has been suspected earlier that oxygen precipitates in silicon in the form of  $\text{SiO}_2$ . In our investigations the validity of this assumption has been verified for the case of large precipitates at dislocations. However, this was done with precipitates which had been obtained from indiffused oxygen, whilst previous investigations related to the precipitation of bulk oxygen, which had been dissolved in the lattice during crystal growth. The results, described here, are however also valid for the precipitation of bulk oxygen. This has been verified in silicon single crystals grown from the melt, whose content of dissolved oxygen had been determined by means of infrared absorption at  $5 \times 10^{17} \text{ cm}^{-3}$ . The dislocation density amounted in this case to about  $10^8 \text{ cm}^{-2}$ . Samples with dimensions  $3.3 \times 3.3 \times 12 \text{ mm}^3$  were first sawn from larger single crystals. Some of these samples were deformed under dynamic pressures up to the lower yield point in order to achieve a higher dislocation density, the pressure axis being oriented in the  $\langle 123 \rangle$  direction. The electron microscopically determined dislocation density amounted in this case to about  $10^8 \text{ cm}^{-2}$ . The deformed and non-deformed samples were then annealed for 24 h at 1000° C in an inert gas atmosphere (argon + 3% hydrogen). The following electron microscope examination showed that in crystals with high

dislocation density, precipitates of the type described above were present. Their number was of course some orders of magnitude smaller than that which arose under the action of external oxygen. This was probably caused by the comparatively smaller oxygen content in the first named samples. On the other hand no precipitates could be detected in the non-deformed samples. This proves that the precipitation of bulk oxygen is favoured by the presence of dislocations.

In semiconductor devices one wishes to avoid these precipitates since they can prove deleterious to voltage breakdown properties. This is because they favour the formations of microplasmas initiated probably as a result of the different permittivities of silicon and SiO<sub>2</sub> [22]. The results of this work demonstrate the necessity of using silicon with a low dislocation density thus inhibiting the formation of SiO<sub>2</sub> precipitates. However, in silicon device manufacture in particular, precipitation will unavoidably take place in the dislocation network produced by e.g. the phosphorus and boron diffusions, due to the misfit of these atoms in the silicon lattice [23].

### Acknowledgement

We wish to thank Professor P. Haasen and J. L. Lambert for helpful discussions. Furthermore we are indebted to Mr H. Baier for his assistance in preparing the samples.

### References

1. H. J. HROSTOWSKI and R. H. KAISER, *Bull. Amer. Phys. Soc.* **2** (1956) 295.
2. W. KAISER, *Phys. Rev.* **105** (1957) 1751.
3. W. KAISER and P. H. KECK, *J. Appl. Phys.* **28** (1957) 882.
4. W. KAISER, P. H. KECK, and C. F. LANGE, *Phys. Rev.* **101** (1956) 1264.
5. W. C. DASH, *ibid* **98** (1955) 1506.
6. G. H. SCHWUTTKKE, *J. Appl. Phys.* **33** (1962) 2760; *J. Electrochem. Soc.* **109** (1962) 27.
7. J. R. PATEL and A. R. CHAUDHURI, *J. Appl. Phys.* **33** (1962) 2223.
8. S. LEDERHANDLER and J. R. PATEL, *Phys. Rev.* **108** (1957) 239.
9. G. L. PEARSON, W. T. READ, and W. L. FELDMANN, *Acta Met.* **5** (1957) 181.
10. J. R. PATEL, B. W. BATTERMANN, *J. Appl. Phys.* **34** (1963) 2716.
11. C. S. FULLER and R. A. LOGAN, *ibid* **28** (1957) 1427.
12. W. KAISER, H. L. FRISCH, and H. REISS, *Phys. Rev.* **112** (1958) 1546.
13. W. CZAJA and J. R. PATEL, *J. Appl. Phys.* **36** (1965) 1476.
14. J. B. WILLIS, unpublished, ref. by R. BULLOUGH and R. C. N. NEWMAN, *Progress in Semiconductors* **7** (1963) 99.
15. R. A. LOGAN, *Phys. Rev.* **100** (1955) 615.
16. A. G. TWEET, *ibid* **106** (1957) 221.
17. H. RIEGER, *Phys. Stat. Sol.* **7** (1964) 685.
18. M. RENNINGER, *Z. angew. Phys.* **19** (1965) 20.
19. W. W. TYLER and W. C. DASH *J. Appl. Phys.* **28** (1957) 1221.
20. G. R. BOOKER and R. STICKLER, *Brit. J. Appl. Phys.* **13** (1962) 446.
21. P. B. HIRSCH, *et al*, "Electron Microscopy of Thin Crystals" (Butterworth, London, 1965).
22. A. GOETZBERGER, *Festkörperprobleme* **3** (1964) 209.
23. S. PRUSSIN, *J. Appl. Phys.* **32** (1961) 1876.